Analysis Methods for Neutral Delay Differential Equations

Griselda R. Itovich
Escuela de Producción, Tecnología
y Medio Ambiente, Sede Alto Valle
Universidad Nacional de Río Negro
Villa Regina, Argentina
Email: gitovich@unrn.edu.ar

Franco S. Gentile
Departamento de Matemática
Universidad Nacional del Sur
Instituto de Investigaciones en
Ing. Eléctrica-IIIE (UNS-CONICET)
Bahía Blanca, Argentina
Email: fsgentile@gmail.com

Jorge L. Moiola
Depto. de Ing. Eléct. y de Comp.
Universidad Nacional del Sur
Instituto de Investigaciones en
Ing. Eléctrica-IIIE (UNS-CONICET)
Bahía Blanca, Argentina
Email: jmoiola@uns.edu.ar

***Abstract*—Two different methods for the stability and bifurcation analyses of neutral delay differential equations are presented. The first one relies on classical techniques and it is oriented to the study of the roots of the characteristic equation, which is a transcendental one. It provides a straightforward test to obtain the stability chart in the parameter space of the studied system. The second method uses a frequency-domain approach, based on the control theory, to determine the stability and dynamic bifurcations, and also providing approximations for the smooth oscillations appearing when the system loses its stability.**

***Index Terms*—neutral delay differential equations, exponential polynomial equations, nonlinear systems, stability, oscillatory solutions.**

I. Introduction

Among the most used equations for modeling systems in engineering and other areas, delay differential equations are of special interest, because they are useful to represent time delays in transmission lines, control loops, switching times, sensing and processing information, *etc*. There are three main types of delay equations: the *retarded* type, the *neutral* type and the *advanced* type [1]. In the first kind, the present rate of change of the system depends on the present and past values of the states, that is to say, the time delay does not appear in the highest-order derivative in the differential equation. In the second kind, the rate of change of the system at present and past time values depends on present and past values of the states. Thus, neutral equations have time delays appearing in the highest-order derivative. At last, in equations of the advanced type, the rate of change of the system at the present time depends on present and future values of the states. More details about the classification of delay equations can be found in [1]. Since equations of retarded type have been widely studied in relation with engineering applications [2], [3], this article focus on the study of equations of the neutral type. Even if the characteristic equation is an exponential polynomial in all delay equations, the stability analysis may be different in each case. For equations of the retarded type, there are classic results showing that the stability changes may only occur when one or more eigenvalues cross the imaginary axis, and there is always a finite number of roots of the characteristic equation in any vertical strip of the complex plane. But this is not generally true for equations of the neutral type. Actually, in neutral delay differential equations (NDDEs), the stability can be lost even without the crossing of characteristic roots through the imaginary axis, because those roots can accumulate on that axis. Those differences seem not to be well known in the engineering community though there are many research works using NDDEs. A numerical method for the stability analysis of NDDEs, which used a special function called the W-Lambert function, was proposed in [4]. The stability and appearance of oscillations in a neural network model described by an NDDE has been studied in [5]. NDDEs arise naturally in some models of transmission lines, described by distributed parameters. For example, an alternative configuration of the Chua's oscillator with a lossless transmission line, described by an NDDE, was investigated in [6]. The Hopf bifurcation and the period-doubling route to chaos was analyzed and observed experimentally in a radio-frequency transmission line in [7], where the system model was also an NDDE. In [8], the authors analyzed an NDDE related with the substructuring method, which is a hybrid (empirical and theoretical) tool to analyze very complex dynamical systems.

This article addresses the study of NDDEs, particularly the stability of their equilibrium points and also the appearance of periodic solutions, when these equilibrium points lose their stability. After linearizing the equation around an equilibrium point, a characteristic equation given by an exponential polynomial is obtained. The investigation of the location of its roots is not a simple task. However, with the aid of some classic results, some conditions on the parameters can be deduced to ensure the stability of the equilibrium point. This viewpoint gives place to the first approach presented in this work. In the other hand, an alternative method emerges after representing the system as a feedback control loop, and performing a frequency-domain stability analysis. In this way, the original formulation presented in [9], [10] can be applied after minor modifications to study NDDEs, where the focus is on the appearance of smooth oscillations, when the equilibrium points become unstable after the variation of a system parameter (which is known as Hopf bifurcation). This is the second approach developed in this article.

ISBN: 978-987-1648-44-3

This paper is organized as follows. In Section II, a stability characterization based on classical techniques is presented with its proof. In Section III, the frequency-domain approach is described, an its application to NDDE is explained through an example. Finally, the conclusions are given in Section IV.

II. Stability analysis using classical techniques

This section deals with the analysis of certain dynamical aspects of the following NDDE:

$$\ddot{x}(t) + \gamma x(t) = \alpha \ddot{x}(t-\tau) + \beta \ddot{x}^2(t-\tau), \tag{1}$$

where $\ddot{x} = d^2x/dt^2, \gamma > 0$, α, $\beta \neq 0$ and $\tau > 0$. System (1) can be thought as an harmonic oscillator with nonlinear delayed feedback, and its structure is similar to others analyzed in [11]. The stability of the equilibrium point $\widehat{x} = 0$ of (1) is studied by the following linearized equation, also considered in [12]:

$$\ddot{x}(t) + \gamma x(t) = \alpha \ddot{x}(t-\tau). \tag{2}$$

Equation (2) with three parameters (counting the delay τ), is explored with the aid of different techniques to discover the behavior of its solutions, under parameter variations.

To analyze the stability of the equilibrium point of (2), it is necessary to find the location of the roots of a certain exponential polynomial. In this regard, the following definitions and results will be used.

Definition 1: Let $p(x, y)$ be a two variable polynomial. Then $P(z) = p(z, e^z) = \sum_{m,n} a_{mn} e^{zm} z^n$ is an exponential polynomial.

Definition 2: Let $P(z)$ be an exponential polynomial. The term $a_{rs} e^{zr} z^s$ is called the principal term of P if $a_{rs} \neq 0$ and, if for each other term $a_{mn} e^{zm} z^n$ with $a_{mn} \neq 0$, it is satisfied $r > m, s > n$, or $r = m, s > n$, or $r > m, s = n$.

Remark 1: It can be proved that if an exponential polynomial $P(z)$ has no principal term, then it has an unbounded number of zeros with arbitrarily large real part [1], [13], [14] *e.g.* $P(z) = e^z - z$.

The next results [1], [14] are required for the stability analysis. In the following theorems, consider $P = P(z)$ be an exponential polynomial with a principal term, where $P(iy) = F(y) + iG(y)$, $y \in \mathbb{R}$.

Notation: The expression FG' means the product of F and G'. So $FG'(y) = F(y)G'(y)$. Idem for $F'G$.

Theorem 1 If all the zeros of P are located on the left half plane then all the zeros of F and G are real, alternating and $FG'(y) - F'G(y) > 0$, for all real value y. ■

Theorem 2 All the zeros of P are located on the left half plane if

I) all the roots of F are real and for each of these zeros the condition $F'G(y) < 0$ is satisfied, or

II) all the roots of G are real and for each of these zeros the condition $FG'(y) > 0$ is satisfied, or

III) all the roots of F and G are real and alternate and the inequality $FG'(y) - F'G(y) > 0$ is valid for at least one value of y. ■

Remark 2: $F(y)$ and $G(y)$ simultaneously zero with $y \neq 0$ is equivalent to the existence of a pair of roots of P that are imaginary pure.

Particularly, for Eqn. (2) the characteristic equation results

$$r^2 + \gamma = \alpha r^2 e^{-r\tau} \iff e^{r\tau}(r^2 + \gamma) - \alpha r^2 = 0.$$

If $z = r\tau$ then follows

$$P(z) = e^z(z^2 + \gamma\tau^2) - \alpha z^2 = 0, \tag{3}$$

and taking $z = iy$, it is possible to write $P(iy) = F(y) + iG(y)$, where

$$\begin{aligned} F(y) &= \cos y(-y^2 + \gamma\tau^2) + \alpha y^2, \\ G(y) &= \sin y(-y^2 + \gamma\tau^2). \end{aligned} \tag{4}$$

The solution of $F(y) = G(y) = 0$ allows to find the critical stability curves in the parameter space. If the solutions of $P(iy) = 0$ are not zero, they come in complex-conjugate pairs, and the stability loss of the equilibrium point leads to the appearance of smooth oscillations in (1). This phenomenon is called Hopf bifurcation in the context of nonlinear systems. Thus, the critical stability curves obtained from (4) will be called the Hopf bifurcation curves of (1), and they can be expressed as

$$\alpha_k(\tau) = (-1)^k \left(1 - \frac{\gamma\tau^2}{k^2\pi^2}\right), \quad k \in \mathbb{N}. \tag{5}$$

By Theorem 2 II), if $FG'(y) > 0$ for any root of G, then the equilibrium results asymptotically stable. From now on, for simplicity, it is fixed $\gamma = 1$.

Due to (4), the roots of G are

$$y_k = k\pi, \quad \hat{y}_{1,2} = \pm\tau. \tag{6}$$

Moreover $G'(y) = \cos y(-y^2+\tau^2) - 2y \sin y$. To be able to use Theorem 2 II), some conditions must be satisfied, namely:

1) F and G cannot share any of their roots, *i.e.*

$$\begin{aligned} F(y_k) &= (-1)^k(-y_k^2 + \tau^2) + \alpha y_k^2 \neq 0, \\ F(\hat{y}_{1,2}) &= \alpha \hat{y}_{1,2}^2 = \alpha\tau^2 \neq 0 \iff \alpha \neq 0. \end{aligned} \tag{7}$$

2) The roots of G must be simple. In this regard,

$$\begin{aligned} G'(y_k) &= (-1)^k(-y_k^2 + \tau^2) \neq 0 \Leftrightarrow y_k^2 \neq \tau^2 \\ &\Leftrightarrow \tau \neq k\pi,\ k \in \mathbb{N}, \\ G'(\hat{y}_{1,2}) &= -2\hat{y}_{1,2} \sin \hat{y}_{1,2} = -2\tau \sin\tau \neq 0 \Leftrightarrow \\ &\tau \neq k\pi,\ k \in \mathbb{N}. \end{aligned} \tag{8}$$

Then, the following outcome, which is the main result of this section, can be proved:

Theorem 3 Consider (3) and (4) with $\gamma = 1, \tau > 0, \alpha \neq 0$, together with $y_k, k \in \mathbb{N}^0$ and $\hat{y}_{1,2}$ given by (6). Assume that

ISBN: 978-987-1648-44-3

the parameters values satisfy (7) and (8). All the roots of P lie on the left half plane if and only if the following parameter conditions are fulfilled:

I) For $0 < \tau < y_1$, it must be

$$\alpha < 0 \quad \text{and} \quad \alpha > -1 + \frac{\tau^2}{\pi^2}.$$

II) For $y_k < \tau < y_{k+1}, k \in \mathbb{N}$, it is required:

a) If k is odd, then

$$\alpha > 0,\ \alpha < -1 + \frac{\tau^2}{k^2\pi^2} \ \text{ and } \ \alpha < 1 - \frac{\tau^2}{(k+1)^2\pi^2}.$$

b) If k is even, then

$$\alpha < 0,\ \ \alpha > 1 - \frac{\tau^2}{k^2\pi^2} \ \text{ and } \ \alpha > -1 + \frac{\tau^2}{(k+1)^2\pi^2}.$$

Proof: $\Rightarrow$ (Necessary condition)

This part is proved using Theorem 1. The roots of G and F should be real and this statement can be satisfied under counting them on certain intervals of the line. It is easy to prove that G has always $4k+2$ roots, in an arbitrary interval $[-2k\pi + \pi/2, 2k\pi + \pi/2]$, for k arbitrarily large, wherever a positive τ is placed. Now, consider the roots of F. For the first case I) let $0 < \tau < y_1 = \pi$. It will be shown that F has also $4k+2$ zeros in the interval $[-2k\pi, 2k\pi]$. As F is even, one can consider $[0, 2k\pi]$ and look for $2k+1$ roots. The zeros of F should alternate with the zeros of G (see (6)) according with Theorem 1. So, it results $F(0) = \tau^2, F(\tau) = \alpha\tau^2, F(\pi) = \pi^2 - \tau^2 + \alpha\pi^2$, and supposing that they have different signs, gives $\alpha < 0$ and $\alpha > -1 + \tau^2/\pi^2$. Now, it is considered any subinterval $[y_j, y_{j+1}]$, where $j \geq 1$.

Set j odd, then $F(y_j) = y_j^2 - \tau^2 + \alpha y_j^2$ and $F(y_{j+1}) = -y_{j+1}^2 + \tau^2 + \alpha y_{j+1}^2$. Clearly $F(y_{j+1}) < 0$ and $F(y_j) > 0$ due to $\alpha > -1 + \tau^2/\pi^2 > -1 + \tau^2/(j^2\pi^2)$. So, there is one root of F in $[y_j, y_{j+1}]$. The same result can be shown analogously for j even. Then F has $2k+1$ roots in $[0, 2k\pi]$ and $4k+2$ in $[-2k\pi, 2k\pi]$ and the proof results now complete for this case. The situations considered in part II) can be demonstrated fitting this argument.

$\Leftarrow$ (Sufficiency condition)

In order to apply Theorem 2 II), it is necessary to check that $FG'(y) > 0$ for each y, an arbitrary root of G (see (6)).

I) The sign of α follows from the requirement of $FG'(\hat{y}_i) > 0, i = 1, 2$. The condition $\alpha < 0$ results from the condition $FG_1'(y_0) > 0$. The main inequality is established by setting $FG'(y_1) > 0$. Then, it can be shown that one can satisfy $F_1G_1'(y_k) > 0$, $k \geq 2$, by holding both inequalities and considering separately the cases k odd or even. Hence, the detailed steps of the proof of this part are shown. Let $0 < \tau < \pi = y_1$. Considering the roots of G (6), the sign of FG' gives

1) For $\hat{y}_{1,2} = \pm\tau$, one has $FG'(\hat{y}_{1,2}) = -2\alpha\tau^3 \sin\tau > 0$ if $\alpha < 0$ (due to $0 < \tau < \pi = y_1$).

2) $FG'(0) = \tau^4 > 0$. It follows that

$$FG'(\pi) = (\pi^2 - \tau^2 + \alpha\pi^2)\underbrace{(\pi^2 - \tau^2)}_{>0} > 0 \Rightarrow \alpha > -1 + \frac{\tau^2}{\pi^2}.$$

Now, it is necessary to prove that if $0 < \tau < \pi = y_1$ then $FG'(y_k) > 0$, $k \geq 2, k \in \mathbb{N}$, under $\alpha < 0$ and $\alpha > -1 + \tau^2/\pi^2$.

Consider $y_k = k\pi$, with k odd. One has

$$FG'(k\pi) = (k^2\pi^2 - \tau^2 + \alpha k^2\pi^2)\underbrace{(k^2\pi^2 - \tau^2)}_{>0} > 0$$
$$\Leftrightarrow \alpha > -1 + \tau^2/(k^2\pi^2),$$

which holds if $\alpha > -1 + \tau^2/\pi^2$.

Now, consider $y_k = k\pi$, with k even. As

$$FG'(k\pi) = (-k^2\pi^2 + \tau^2 + \alpha k^2\pi^2)\underbrace{(-k^2\pi^2 + \tau^2)}_{<0} > 0$$
$$\Leftrightarrow \alpha < 1 - \tau^2/(k^2\pi^2),$$

that holds if $\alpha < 0$.

II) Again, the sign of α is established from $FG'(\hat{y}_i) > 0, i = 1, 2$, according to k being odd or even. The first two inequalities in a) and b) are deduced imposing $FG'(y_k) > 0$ and $FG'(y_{k+1}) > 0$, when k is odd or even. These conditions result sufficient to guarantee $FG'(y_i) > 0$, where $i < k$ or $i > k+1$. Finally, to show this last it is necessary to consider the four different cases which result for i odd or even.

It still remains to test that $FG'(y_k) > 0$ for each y_k, a root of G where $y_k < 0$. Due to FG' is an even function, *i.e.*, $FG'(-y_k) = FG'(y_k)$, now the proof is complete.■

The stability regions for system (2), attained by Theorem 3 are shown in Figure 1. Notice that for $|\alpha| = 1$, if $\tau \to 0^+$, there is an accumulation of Hopf bifurcation points (only the Hopf curves up to $k = 7$ are shown in the diagram). It indicates that there are infinitely many solutions of $P(iy) = 0$ for those parameter values. This fact can also be seen from (3) by letting $\tau \to 0^+$ and $|\alpha| = 1$ therein. It results in $P(z) = z^2(e^z \pm 1) = 0$, which has an infinite number of solutions on the imaginary axis. As mentioned in Section I, this is a distinctive feature of NDDEs.

Remark 3: It is also possible to consider τ as a constant. In this situation the stability regions can be set for the parameters α and γ and the restrictions result linear. This approach has been considered in [12]. The outcomes presented in this paper agree with the results therein.

Remark 4: Notice that the results obtained in this section are valid not only for system (1), but also for any system whose linearised equation is given by (2).

III. Stability and bifurcation analysis using a frequency-domain approach

In this section, the frequency-domain approach to the Hopf bifurcation [9], [10] is considered in order to determine the stability and the onset of oscillations in NDDEs. The procedure is introduced directly by considering as example, the equation proposed in [15], given by:

$$\dot{x}(t) = a\dot{x}(t-1) + bx(t-1) + c\dot{x}^3(t-1), \qquad (9)$$

where $x, a, b, c \in \mathbb{R}$. By applying the Laplace transform in both sides, it yields

$$\mathcal{L}\{\dot{x}(t) - bx(t-1)\} = \mathcal{L}\left\{a\dot{x}(t-1) + c\dot{x}^3(t-1)\right\},$$

ISBN: 978-987-1648-44-3

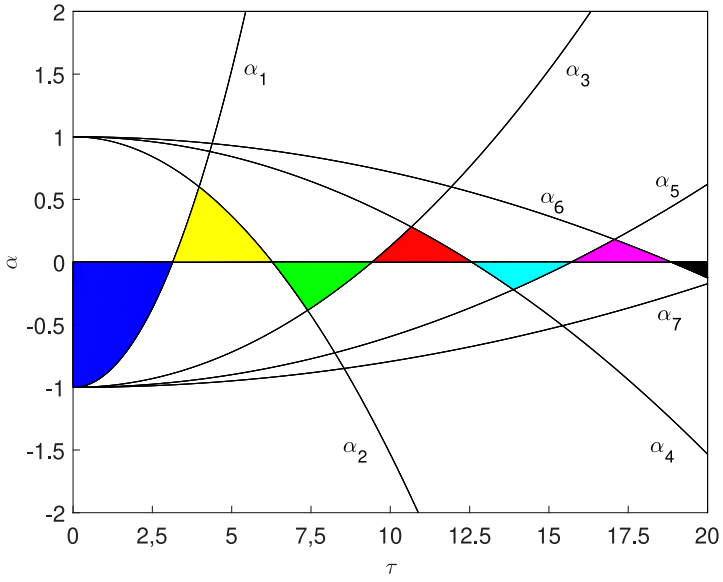

Fig. 1. Some stability regions for the equilibria of model (2) given by Theorem 3. The blue area refers to the region defined in I) and, the yellow, red and magenta areas correspond to part II) a, when $k = 1, 3, 5$ and finally, the green, cyan and black (only a portion), refer to part II) b, with $k = 2, 4, 6$. The curved frontiers of the coloured zones are Hopf bifurcation curves α_k.

which gives

$$\mathcal{L}\{x(t)\} = X(s) = \frac{1}{s - be^{-s}} \mathcal{L}\left\{a\dot{x}(t-1) + c\dot{x}^3(t-1)\right\},$$

so one can write (9) as a linear system G with a nonlinear feedback g which are given, respectively, by

$$G(s) = \frac{1}{s - be^{-s}} \quad \text{and} \quad g(y) = -ay - cy^3.$$

Note, however, that the output of the linear system should be $y(t) = -\dot{x}(t-1)$ instead of $-x(t)$ as in the standard formulation of the frequency-domain approach (see [10]), so an additional block must be added to the forward path, as shown in Fig. 2. Thus the complete transfer function for the linear feedforward path is defined conveniently as $G^*(s) = G(s)se^{-s}$. The equilibrium points $\widehat{y}$ satisfy the equation $G^*(0)g(\widehat{y}) = -\widehat{y}$, which gives the solution $\widehat{y} = 0$. In order to study the stability of this equilibrium point, it is computed the linearization of g around $\widehat{y} = 0$, given by $J = dg/dy|_{y=0} = -a$. Thus one should consider the so-called characteristic function defined by

$$\lambda(s) = G^*(s)J = \frac{-ase^{-s}}{s - be^{-s}}, \tag{10}$$

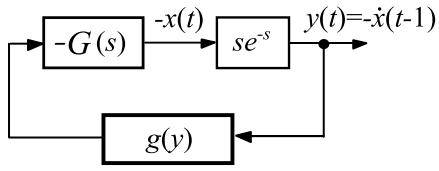

Fig. 2. Block diagram for system (9).

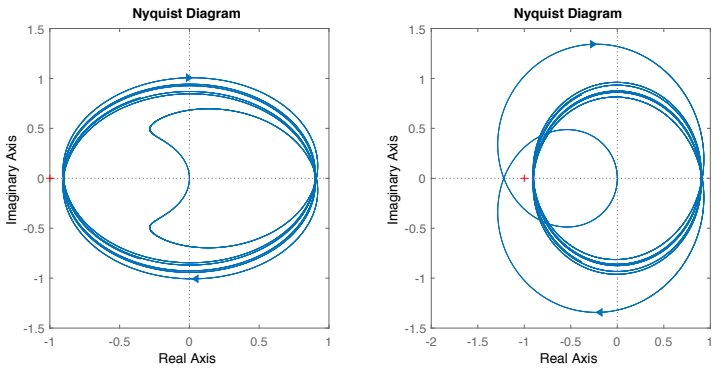

Fig. 3. Nyquist diagrams for system (9), with $a = 0.9$. Left: $b = 0.5$. Right: $b = -0.5$.

which represents the linear loop gain of the system shown in Fig. 2. The function (10) can be used to analyze the stability and bifurcations of the equilibrium point when the Nyquist stability criterion is applied. As in Section II, it is possible to formulate a new result using the time domain formulation, *i.e.*, the adaptation of Theorem 3 to model (9). It can be proved that the conditions $-y_0\sqrt{1-a^2} < b < 0$ where $-1 < a < 1$ and $y_0 = \arccos a$, $y_0 \in (0, \pi)$ are necessary and sufficient to guarantee the asymptotic stability of the equilibrium.

In the following, $a \neq 0$ is supposed in order to the direct transfer function be well defined. Particularly, the Hopf bifurcation phenomena introduced in Section II, is detected in this frequency-domain framework when the condition $\lambda(i\omega_0) = -1$ is satisfied with $\omega_0 \neq 0$. This condition, applied to (10) gives $ai\omega e^{-i\omega} = i\omega - be^{-i\omega}$, or equivalently $b + ia\omega = i\omega e^{i\omega}$, which leads to the following equations after taking real and imaginary parts:

$$b = -\omega \sin \omega \tag{11a}$$

$$a\omega = \omega \cos \omega. \tag{11b}$$

System above has a solution $\omega = 0$ with $b = 0$, indicating the presence of a so-called *static* bifurcation for this parameter value. Generally, a static bifurcation indicates the interaction between more than one equilibrium point, but in this example, there are no more of such points.

On the other hand, (11b) gives $|a| \leq 1$ if $\omega \neq 0$. If $|a| = 1$, then $\omega = k\pi$, $k \in \mathbb{N}$ and it gives again $b = 0$. Thus, discarding $b = 0$ and $|a| = 1$, it yields

$$\omega_0 = \frac{|b|}{\sqrt{1-a^2}}, \quad (b \neq 0,\ |a| < 1). \tag{12}$$

In addition, $\lambda(i\omega)$ can be written as

$$\lambda(i\omega) = \frac{-a\omega^2 \cos\omega + ia\omega(b + \omega \sin\omega)}{|i\omega - be^{-i\omega}|^2},$$

thus if (11a) holds, one has $\mathrm{Im}\lambda = 0$. But (11a) has infinitely many solutions for $b \neq 0$, and it means that λ intersects the real axis infinitely many times. Figure 3 shows two Nyquist diagrams ($a = 0.9$): one for $b = 0.5$ (left) and the other for $b = -0.5$ (right). The plot on the right shows the occurrence of a Hopf bifurcation, since the geometrical locus encloses the

ISBN: 978-987-1648-44-3

point -1. Also, if $|a| = 1$, then the characteristic locus passes through the critical point -1 an infinite number of times. Note that for $|a| = 1$ there is an accumulation of roots on the imaginary axis in the time-domain counterpart, as happened for the system studied in Section II.

Since (9) has a nonlinearity, the Hopf bifurcation theorem provides a formula, called curvature coefficient, to determine the direction and stability of oscillations. An approximation of the limit cycles following the method [10] with two harmonics, gives that the zero and second harmonic terms vanish, since $D^2g = d^2g/dy^2|_{\widehat{y}=0} = 0$. Also, as the system is SISO (single input - single output), the left and right eigenvectors u and v of $G^*(s)J$ are scalar and they can be chosen as one. Thus, the amplitude of the fundamental frequency component is proportional to the following quantity, provided in a simplified form using the fact that $D^2g = 0$:

$$p_1(\omega) = \frac{1}{8}\frac{d^3g}{dy^3}\bigg|_{\widehat{y}=0} v = \frac{1}{8}(-6c)\, v = -\frac{3c}{4},$$

and then one obtains an auxiliar complex scalar

$$\xi_1(\omega) = -G^*(\omega)p_1(\omega) = \frac{3c}{4}\frac{i\omega e^{-i\omega}}{(i\omega - be^{-i\omega})}, \qquad (13)$$

which helps in a graphical interpretation presented in short. Using the fact that $u = v = 1$, the expression of the above mentioned curvature coefficient is reduced to

$$\sigma_1 = \mathrm{Re}\left\{\xi_1(i\omega_0)[G^{*\prime}(i\omega_0)J]^{-1}\right\}, \qquad (14)$$

where $\mathrm{Re}(\cdot)$ is the real part of a complex number and $G^{*\prime}(i\omega_0) = dG^*(s)/ds|_{s=i\omega_0}$. The sign of this coefficient determines if the Hopf bifurcation is supercritical (the oscillation appears beyond the critical parameter value) or subcritical (the periodic solution emerges before the critical value). Replacing the expressions of $G^{*\prime}(i\omega_0)$ and $\xi_1(\omega_0)$ into (14), one obtains

$$\sigma_1 = \frac{3c}{4a}\mathrm{Re}\left\{i\omega_0(i\omega_0 - be^{-i\omega_0})[be^{-i\omega_0} - \omega_0^2]^{-1}\right\}. \qquad (15)$$

The expression above can be further simplified by using the critical bifurcation condition $\lambda(i\omega_0) = -1$, which is equivalent to $i\omega_0 - be^{-i\omega_0} = ai\omega_0 e^{-i\omega_0}$. Using this into (15), after some algebraic manipulation, gives

$$\sigma_1 = -\frac{3c\omega_0^2}{4}\left\{\frac{b - \omega_0^2\cos\omega_0}{|-\omega_0^2 e^{i\omega_0} + b|^2}\right\}.$$

Finally, replacing ω_0 from (12) and $\cos\omega_0 = a$ from (11b), expression above can be further simplified to

$$\sigma_1 = -\frac{3c\omega_0^2 b}{4(1-a^2)}\left\{\frac{(1 - a^2 - ab)}{|-\omega_0^2 e^{i\omega_0} + b|^2}\right\}. \qquad (16)$$

As $1 - a^2 > 0$, the Hopf bifurcation will be supercritical if $cb[1 - a^2 - ab] > 0$ and subcritical if $cb[1 - a^2 - ab] < 0$.

The Hopf bifurcation curves obtained from (11a) and (11b) are shown in Fig. 4. Each portion of the curve corresponds to $(k-1)\pi < \omega < k\pi$, and they are shown only for k up to six.

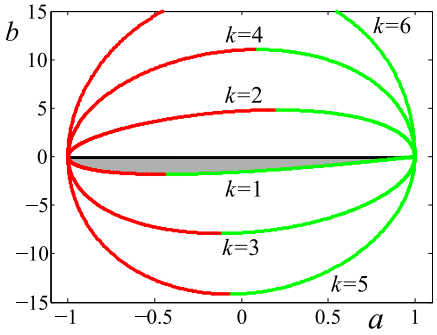

Fig. 4. Hopf bifurcation curves. Supercritical bifurcations are shown in red and subcritical ones are shown in green. Each portion corresponds to $(k-1)\pi < \omega < k\pi$, and the shaded area corresponds to a stable equilibrium.

Red color indicates supercritical Hopf bifurcations, and green color indicates subcritical Hopf bifurcations. In each portion, there is a point in which the curvature coefficient vanishes. For $k = 1$, the point for which $\sigma_1 = 0$ coincides with the one found in [15] using a different method (see Table 3.1 therein).

On the other hand, the amplitude and frequency of the periodic solutions can be obtained approximately by solving the equation

$$\lambda(i\omega) = -1 + \xi_1(\omega)\theta^2, \qquad (17)$$

which can be interpreted graphically as the intersection, in the complex plane, between the characteristic function λ and the half-line starting from -1, and pointing to the direction of ξ_1. This half-line is parametrized in θ^2, where θ is a measure of the amplitude of the periodic solution. By replacing (10) and (13) into (17), it is simple to obtain $-ai\omega = -i\omega e^{i\omega} + b + \frac{3}{4}ci\omega\theta^2$, leading to the system

$$b = -\omega\sin\omega, \qquad (18a)$$

$$a = \cos\omega - \tfrac{3}{4}c\theta^2. \qquad (18b)$$

For each value of b, the intersecting frequency $\widehat{\omega}$ can be obtained from (18a). Then the amplitude is computed using (18b). For example, with $c > 0$, it gives

$$\theta = \tfrac{2}{\sqrt{3c}}\sqrt{\cos\widehat{\omega} - a}.$$

The periodic solution in terms of the output of the linear subsystem is then computed as $y(t) = \mathrm{Re}(\theta e^{i\widehat{\omega}t}) = \theta\cos(\widehat{\omega}t)$, but given the relationship $y(t) = -\dot{x}(t-1)$, it follows that $x(t) = -\int_0^t y(u+1)du$, so, by ignoring the time shift (because one is considering the long-term behavior), it is found that $x(t)$ can be expressed as

$$x(t) = -\frac{\theta}{\widehat{\omega}}\sin(\widehat{\omega}t) = \frac{-2}{\widehat{\omega}\sqrt{3c}}\sqrt{\cos\widehat{\omega} - a}\,\sin(\widehat{\omega}t) \quad (c > 0).$$

Next, the obtained approximation will be checked by assigning particular parameter values, and letting one free bifurcation parameter.

Case 1

Consider, as a particular case, $a = 1/\sqrt{2}$, $c = 0.1$ and let

ISBN: 978-987-1648-44-3

b to be the bifurcation parameter. The critical values of b and ω are found from (11a) and (11b) as $b_0 = -\pi/(4\sqrt{2})$, and $\omega_0 = \pi/4$. If b is increased from this critical value, a periodic solution is found. Figure 5 shows the approximation of the branch of periodic solutions. Notice that the Hopf bifurcation is subcritical with unstable periodic solutions. Then, they cannot be observed by standard numerical simulations. However, the obtained amplitude values are slightly higher than those shown in [15] for the same branch using a different methodology.

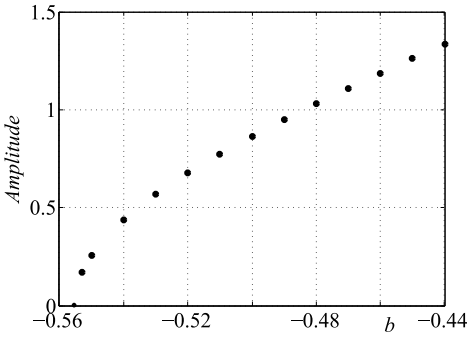

Fig. 5. Approximation of the branch of periodic solutions emerging from the Hopf point $(a, b) = (1/\sqrt{2}, -\pi/(4\sqrt{2}))$.

Case 2

Consider now $a = -1/\sqrt{2}$ (obtained for $\omega_0 = 3\pi/4$), $c = 0.1$ and let b to be again the bifurcation parameter. The critical value of b is found from (11a) to be $b_0 = -3\pi/(4\sqrt{2})$. Now b is decreased from this critical value, taking into account that the Hopf bifurcation is supercritical in this case. Figure 6 shows the comparison between the amplitude of the emerging stable limit cycles found with numerical simulations and those predicted by the graphical Hopf theorem. It can be seen that the latter can detect the proximity of a saddle-node bifurcation of limit cycles.

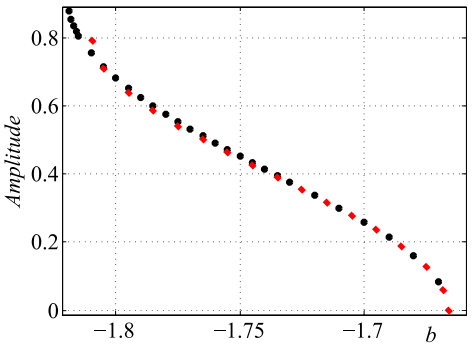

Fig. 6. Approximation of the branch of periodic solutions emerging from the Hopf point $(a, b) = (-1/\sqrt{2}, -3\pi/(4\sqrt{2}))$ (black marks) versus the amplitude computed through numerical simulations (red marks).

Remark 6: The nonlinear system (1) can be also analyzed by using the frequency-domain approach. In so doing, one possible representation is given by $G^*(s) = \frac{s^2 e^{-s\tau}}{s^2+\gamma}$ and $g(y) = -\alpha y + \beta y^2$. Thus, the stability conditions for the equilibrium point obtained in Section II, can be also derived by applying the Nyquist stability criterion to the characteristic function $\lambda(s) = -\alpha s^2 e^{-s\tau}/(s^2 + \gamma)$.

IV. Conclusion and Future Work

In this work, two approaches were presented for the stability and bifurcation analyses of two particular NDDEs, with the intention of extending those results to more general cases in future developments. Based on Theorems 1 and 2, similar results to Theorem 3 can be set for more general NDDEs, performing a similar analysis as in the proof of Theorem 3. Also, it seems to be straightforward to extend the second approach to other systems. Moreover, from the periodic branch shown in Fig. 6, it is glimpsed the appearance of folds of limit cycles, which is expected given the presence of points in which the curvature coefficient vanishes. The fold of limit cycles is a global phenomena, but it can still be recovered using higher-order approximations of the periodic solution, which is left for future work.

Acknowledgments

This work was supported by Universidad Nacional de Río Negro (PI 40A623), Universidad Nacional del Sur (PGI 24/K087), ANPCyT (PICT 2014-2161) and CONICET (PIP 112-201201-00144).

References

[1] R. Bellman and K. Cooke, *Differential-Difference Equations*, Academic Press, New York, 1963.
[2] R. Sipahi, S. I. Niculescu, C. T. Abdallah, W. Michiels and K. Gu "Stability and stabilization of systems with time delay," *IEEE Control Syst. Mag.* 31, 38–65 (2011).
[3] H. Y. Hu and Z. H. Wang, *Dynamics of Controlled Mechanical Systems with Delayed Feedback*, Springer, New York, 2002.
[4] Z. H. Wang "Numerical stability test of neutral delay differential equations," *Math. Problems in Engineering* Art. 698043, 10 pages (2008).
[5] M. Liu, Z. Zhang and X. Xu "Dynamics of a class of neutral three neurons network with delay," *Advances in Diff. Eqns.* 2013, 2013:338 (2013).
[6] X. Liao "Dynamical behavior of Chua's circuit with lossless transmission line," *IEEE Trans. on Circuits and Systems* 63, pp. 245–255 (2016).
[7] J. N. Blakely and N. J. Corron, "Experimental observation of delay-induced radio frequency chaos in a transmission line oscillator", *Chaos* 14(4), pp. 1035–1041 (2004).
[8] Y. M. Kyrychko, K. B. Blyuss, A. Gonzalez-Buelga, S. J. Hogan and D. J. Wagg "Real-time dynamic substructuring in a coupled oscillator-pendulum system," *Proc. of the Royal Soc. A* 462, pp. 1271–1294 (2006).
[9] A. I. Mees and L. O. Chua, "The Hopf bifurcation theorem and its applications to nonlinear oscillations in circuits and systems", *IEEE Trans. on Circuits and Systems* 4, pp. 235–254 (1979).
[10] J. L. Moiola and G. R. Chen, *Hopf Bifurcation Analysis: A Frequency-Domain Approach*, World Scientific, Singapore, 1996.
[11] G. R. Itovich, F. S. Gentile and J. L. Moiola "Hybrid methods to study stability and bifurcations in delayed feedback systems," *Int. J. of Bifurcation and Chaos*, in press, to appear in November 2019.
[12] G. Stépán, *Retarded Dynamical Systems: Stability and Characteristic Functions*, Pitman Research Notes in Mathematics Series, Vol. 210, Longman, UK, 1989.
[13] L. S. Pontryagin, "On the zeros of some elementary trascendental functions," *America Math. Society Tanslations* 21(1), pp. 95-110 (1955).
[14] R. Bellman and J. Danskin Jr., "A Survey of the Matematical Theory of Time-Lag, Retarded Control and Hereditary Processes", *Report 256, The Rand Corporation*, California (1954).
[15] L. Zhang and G. Stépán, "Hopf bifurcation analysis of scalar implicit neutral delay differential equation", *Electronic J. of Qualitative Theory of Diff. Eqns.* 62, pp. 1–9 (2018).

ISBN: 978-987-1648-44-3